Hashmi, Syed Ghufran; Halme, Janne; Saukkonen, Tapio; Rautama, Eeva-Leena; Lund, Peter

# High performance low temperature carbon composite catalysts for flexible dye sensitized solar cells

*Published in:*
Physical Chemistry Chemical Physics

*DOI:*
10.1039/c3cp52982g

Published: 01/01/2013

*Document Version*
Peer-reviewed accepted author manuscript, also known as Final accepted manuscript or Post-print

*Please cite the original version:*
Hashmi, S. G., Halme, J., Saukkonen, T., Rautama, E.-L., & Lund, P. (2013). High performance low temperature carbon composite catalysts for flexible dye sensitized solar cells. *Physical Chemistry Chemical Physics*, *15*(40), 17689-17695. https://doi.org/10.1039/c3cp52982g

PCCP

# Accepted Manuscript

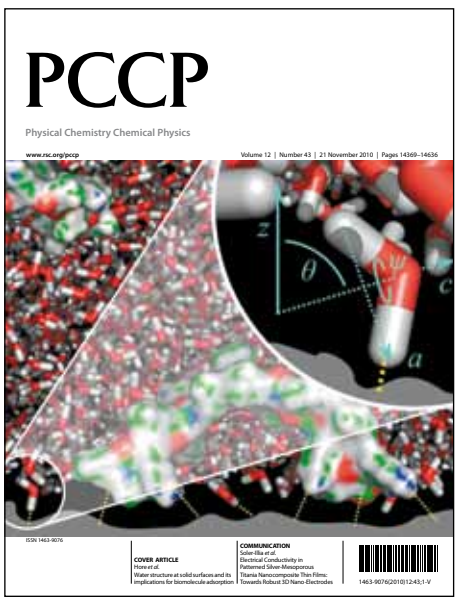


This is an *Accepted Manuscript*, which has been through the RSC Publishing peer review process and has been accepted for publication.

*Accepted Manuscripts* are published online shortly after acceptance, which is prior to technical editing, formatting and proof reading. This free service from RSC Publishing allows authors to make their results available to the community, in citable form, before publication of the edited article. This *Accepted Manuscript* will be replaced by the edited and formatted *Advance Article* as soon as this is available.

To cite this manuscript please use its permanent Digital Object Identifier (DOI®), which is identical for all formats of publication.

More information about *Accepted Manuscripts* can be found in the **Information for Authors**.

Please note that technical editing may introduce minor changes to the text and/or graphics contained in the manuscript submitted by the author(s) which may alter content, and that the standard **Terms & Conditions** and the **ethical guidelines** that apply to the journal are still applicable. In no event shall the RSC be held responsible for any errors or omissions in these *Accepted Manuscript* manuscripts or any consequences arising from the use of any information contained in them.

# High performance low temperature carbon composite catalysts for flexible dye sensitized solar cells

*Syed Ghufran Hashmi* [a*], *Janne Halme* [a], *Tapio Saukkonen* [b], *Eeva-Leena Rautama* [c] *and Peter Lund* [a]

[a] New Energy Technologies Group, Department of Applied Physics, Aalto University, P.O. BOX 15100, FI-00076 Aalto (Espoo), Finland

[b] Engineering Materials Group, Department of Engineering Design and Production, Aalto University (Espoo), Finland

[c] School of Chemical Technology, Department of Chemistry, Aalto University (Espoo), Finland

* Corresponding author: Telephone: +358505952671

E-mail address: ghufran.hashmi@aalto.fi, sghufranh28@gmail.com

**Abstract**

Roll-to-roll manufacturing of dye sensitized solar cells (DSSC) requires efficient and low cost materials that adhere well on the flexible substrates used. In this regard, different low temperature carbon composite counter electrode (CE) catalyst ink formulations for flexible DSSC were developed that can be simply and quickly coated on plastic substrates and dried below 150 °C. The CEs were investigated in terms of photovoltaic performance in DSSC by current-voltage measurement, mechanical adhesion properties by bending and tape tests, electro-catalytic performance by electrochemical impedance spectroscopy and microstructure by electron microscopy. In the bending and tape tests, PEDOT-carbon composite catalyst layer exhibited higher elasticity and better adhesion on all the studied substrates (ITO-PET and ITO-PEN plastic, and FTO-glass), compared to a binder free carbon composite and a $TiO_2$ binder enriched carbon composite, and showed lower charge transfer resistance (1.5 – 3 $\Omega cm^2$) than the traditional thermally platinized CE (5 $\Omega cm^2$), demonstrating better catalytic performance for the tri-iodide reduction reaction. Also the $TiO_2$ binder enriched carbon composite showed good catalytic characteristics and relatively good adhesion on ITO-PET, but on ITO-PEN its adhesion was poor. A DSSC with the $TiO_2$ binder enriched catalyst layer reached 85% of the solar energy conversion efficiency of the reference DSSC based on traditional thermally platinized CE. Based on the aforementioned characteristics, these carbon composites are promising candidates for replacing the platinum catalyst in a high volume roll-to-roll manufacturing process of DSSCs.

**Keywords:** Counter electrode, carbon composite, screen printing, low temperature

## 1. Introduction

Dye sensitized solar cells (DSSC) have a major potential for low-cost and roll-to-roll manufacturing [1]. Efforts have been made to replace the traditional high cost materials of DSSC such as rigid conducting glass with low cost polymer substrates [2-5]. However, the use of polymers is restricted by the temperatures encountered in the preparation of the cells.

Additionally a standard DSSC utilizes platinum (Pt) as a catalyst layer [6-8] to increase the rate of the tri-iodide ion reduction reaction, but it is also another expensive component of the cell [1, 9]. Together with cheap substrates, alternative low priced catalysts could pave the way for reducing the cost of a complete DSSC. Carbon as an alternative catalyst in various structures offers interesting approach to address the problem [10-14].

Previous studies have demonstrated the viability of carbon for use as a counter electrode (CE) in DSSC [1, 12-14]. Also the carbon nanomaterials exhibited remarkable catalytic performance with alternative redox couples such as $Co(L)_2^{2+/3+}$ on Fluorine doped tin oxide (FTO) glass due to their better catalytic performance than the traditional $I^-/I_3^-$ redox couple [15] and can be realized in implementing with the flexible substrates as well. High temperature fabrication processes can be used to fabricate the carbon composites for different cell designs, for instance, rigid monolithic cell type assemblies [13, 14], or flexible metallic sheets in which the cell is sintered after deposition of carbon to increase the adhesion with the substrate [14, 16].

The fabrication of DSSC on plastic sheets, for instance indium-doped tin oxide polyethyleneterephtalate (ITO-PET) and indium-doped tin oxide polyethylenenaphtalate (ITO-

PEN, is restricted by the deformation limit of these plastics which is ca. 150 °C [9]. It is therefore highly justified to develop low-temperature inks or pastes to avoid a post-sintering step typical in the standard fabrication process of DSSC on FTO-glass. Presently, low-temperature deposition of carbon composites suitable for plastic-based CEs has still shortcomings in adhesion and bending properties, e.g. when applied on flexible polymer substrates [1, 17].

We present here a comparative analysis of low temperature carbon composite catalyst layers for DSSC deposited on FTO coated glass, ITO-PEN and ITO-PET sheets together with a glass-based photoelectrode (PE). Parameters determined include mechanical stability, photovoltaic efficiency and charge transfer performance. We were able to demonstrate a high-performance and highly flexible CE based on a carbon-composite catalyst with a much lower charge transfer resistance (1.5 - 3 $\Omega cm^2$) than in thermally platinized CEs (~ 5 $\Omega cm^2$) which had a positive effect on the overall efficiency of DSSC.

## 2. Experimental methods

### *2.1 Fabrication of photoelectrode (PE)*

The photoelectrodes (PEs) for this study were prepared as follows:

Fluorine doped tin oxide (FTO) coated glass substrates (Sheet resistance 15 Ω/□, Hartford Glass Company, Inc) were first cleaned with the detergent, sonicated in the ethanol and acetone solutions (3 min each) and then dried with compressed air. The substrates were then placed in a UV-$O_3$ Chamber (Bio-force nano sciences UV Ozone Pro Cleaner) for 20 minutes and were quickly transferred into a 40 mM $TiCl_4$ solution container and heated for 30 minutes at 70 °C. The substrates were then rinsed with deionized water and ethanol respectively and were dried at

room temperature. After that they were placed in an oven and sintered at 450 °C and then cooled down to room temperature. An 8-10 μm thick layer of commercial nano-crystalline $TiO_2$ paste (18NR-T Dyesol) was printed by screen printing with mesh T-61 and dried at 110°C. After that 2-4 μm thick layer of $TiO_2$ scattering paste (WER2-0 Dyesol) was deposited by screen printing (mesh T-61) and again dried at 110 °C for 5 minutes. The deposited layers were then sintered at 450 °C for 30 minutes and were cooled down to room temperature. The substrates were immersed once again in the 40 mM $TiCl_4$ solution at 70 °C for additional 30 minutes. Consequently the second time $TiCl_4$ treated substrates were again sintered at 450 °C and were cooled down to room temperature to complete the process. The photoelectrodes (PEs) were then sensitized in a 0.32 mM cis bis (isothiocyanato) bis (2, 20-bipyridyl-4, 40-dicarboxylato)-ruthenium (II) bis tetrabutylammonium (N-719, Solaronix) in ethanol (99.5 wt %) for 16 hours.

*2.2 Counter electrodes (CE)*

The counter electrodes (CEs) were prepared as follows:

Thermal Platinization

4 μl of 5 mM solution of choloroplatinic acid hydrate ($H_2PtCl_4.6H_2O$) in 2-Propanol was spread on FTO glass and fired at 390 °C for 20 minutes to complete the process. The substrates were cooled down to room temperature and were kept in a closed plastic box before use.

Carbon composites based catalyst layers were deposited on FTO coated glass (sheet resistance 15 Ω/□), ITO-PEN (15 Ω/□) and ITO-PET (60 Ω/□) substrates by doctor blading.

Details of carbon composite based pastes

1.2 g of graphite powder (particle size 1-5 μm (Sky Spring Nanomaterials Inc) was first mixed with 0.4 g of carbon furnace black particles (20 nm Printex L6) and 0.4 g of Sb:$SnO_2$ (Zelec ECP 3010-XC, Milliken Chemicals). The graphite powder and Sb:$SnO_2$ are used to promote the electrical conductivity of the film and to function as conducting binding particle respectively whereas the furnace black nano-powder was introduced to act as the primary catalyst particle due to its high specific surface area. The composite is then dispersed in 8-10 ml of water and t-butanol solution (1:1), grinded in a ball mill for 2 hours and collected in a clean vial as a binder free carbon composite (BFCC). For PEDOT carbon composite (PCC) the same composition (as mentioned above) was grinded in the ball mill for 2 hours and collected in another vial. After that 2 ml of PEDOT PSS solution (Sigma Aldrich) was added into the composite and stirred for 15 minutes. The PEDOT was added mainly to act as an additional catalyst, but also to possible improve the film conductivity and adhesion. The binder enriched carbon composite (BCC) was obtained by adding 0.4 g of $TiO_2$ as an additional binder in the above mentioned composite composition before milling in water and t-butanol solution.

*2.3 Cell assemblies*

A sandwich type of cell assembly was fabricated by separating the PE and CE with a 50 μm thick Bynel foil (Dupont). The thickness for the carbon composite counter electrodes were adjusted to 20-30 μm. The high stability electrolyte containing $I^-/I_3^-$ redox couple and methoxypropionitrile solvent (EL-HSE) from Dyesol was injected via drilled holes at PE. The holes were then sealed with a 25 μm thick Bynel foil (Dupont) and thin glass cover. Copper tape and silver ink were then applied onto the non-active area of the cell to make the contacts and

were protected with a slow drying epoxy. Before measurements, the cells were soaked for 1 day under 1 sun light intensity (1000 W/m$^2$) for initial stabilization.

*2.4 CE-CE cell configuration*

The CE-CE cell was constructed by depositing each type of carbon composite on FTO-glass ($R_{SH}$ = 15 Ω/□) with symmetrical geometry (area = 0.4 cm$^2$). The thickness of the deposited catalyst layers was adjusted to 20-30 μm with doctor blading. The glass electrodes were separated with 80 μm thick Bynel foil. The electrolyte is then injected via drilled holes in one electrode. The holes were sealed with 25 μm cover foil and a thin glass cover.

*2.5 SEM imaging*

The samples for scanning electron microscopy were prepared on ITO-PET plastic and the images were recorded with Zeiss Ultra 55 FEG-SEM scanning electron microscope equipped with Bruker AXS energy dispersive analyzer (EDS) which was used to detect the particles of composites.

*2.6 Measurements*

The IV curves were measured in a solar simulator under a 1000 W/m$^2$ light intensity equivalent to 1 Sun. An electrochemical impedance spectrum analyzer (Zahner-Elektrik IM6 potentiostat) was used to measure the electrochemical impedance spectra (EIS) of the samples. Film thicknesses were measured with Dektak 6M stylus profiler.

## 3. Results and Discussions

### *3.1 Morphology of catalyst layers*

Figure 1 represents the SEM images of three different composites deposited on ITO-PET plastic: binder free carbon composite BFCC (a, b), PEDOT carbon composite PCC (c, d) and binder enriched carbon composite BCC (e, f) which were described earlier in Section 2. Some of the materials used in the composites can be identified in Figures 1a, and 1b. Additionally, the EDS spectrum of each type of composite has been provided in the supplementary information (See Supporting Information), whereas Figures 1b, 1d and 1f provide details of the morphological structures.

The composite layers have completely covered the large FTO crystals that can be seen in Fig. 1g. All layers look highly porous compared to the thermally platinized catalyst layer in Fig. 1h and contain agglomerates of $SnO_2$, furnace (carbon) black and $TiO_2$ nanoparticles (10-40 nm). Carbon in the form of graphite and furnace black can be distinguished in the SEM images as darker particles compared to the $SnO_2$ and $TiO_2$ particle clusters that appear brighter due to higher atomic weight. This interpretation was confirmed by EDS analysis. However, due to the small size and similar shapes and atomic weights the $SnO_2$ and $TiO_2$ particles could not be reliably distinguished in the SEM images and are hence labeled "$SnO_2$ or $TiO_2$" in the figures. However, their overall presence could be confirmed by EDS (Supporting Information). The graphite crystals that are used to enhance conductivity of the film are much larger in size (2-4 μm) than these nanoparticles and are randomly distributed all across the layer (Fig.1 a, b, e and f). Additionally clusters of $SnO_2$, furnace black and $TiO_2$ nano-particles are stacked over graphite crystals suggesting a higher surface area compared to a thermally platinized catalyst layer (Fig.1

h) which is a key requirement for a good catalyst layer. The thermal platinization produced very small (2 nm) Pt particles distributed all over the large FTO crystals (Fig.1 h). Based on these observations, a lower charge transfer resistance in carbon based composites could be expected compared to thermally platinized counter electrodes provided that films are conductive enough and are made thick enough to compensate for the lower intrinsic catalytic activity of carbon compared to Pt [17].

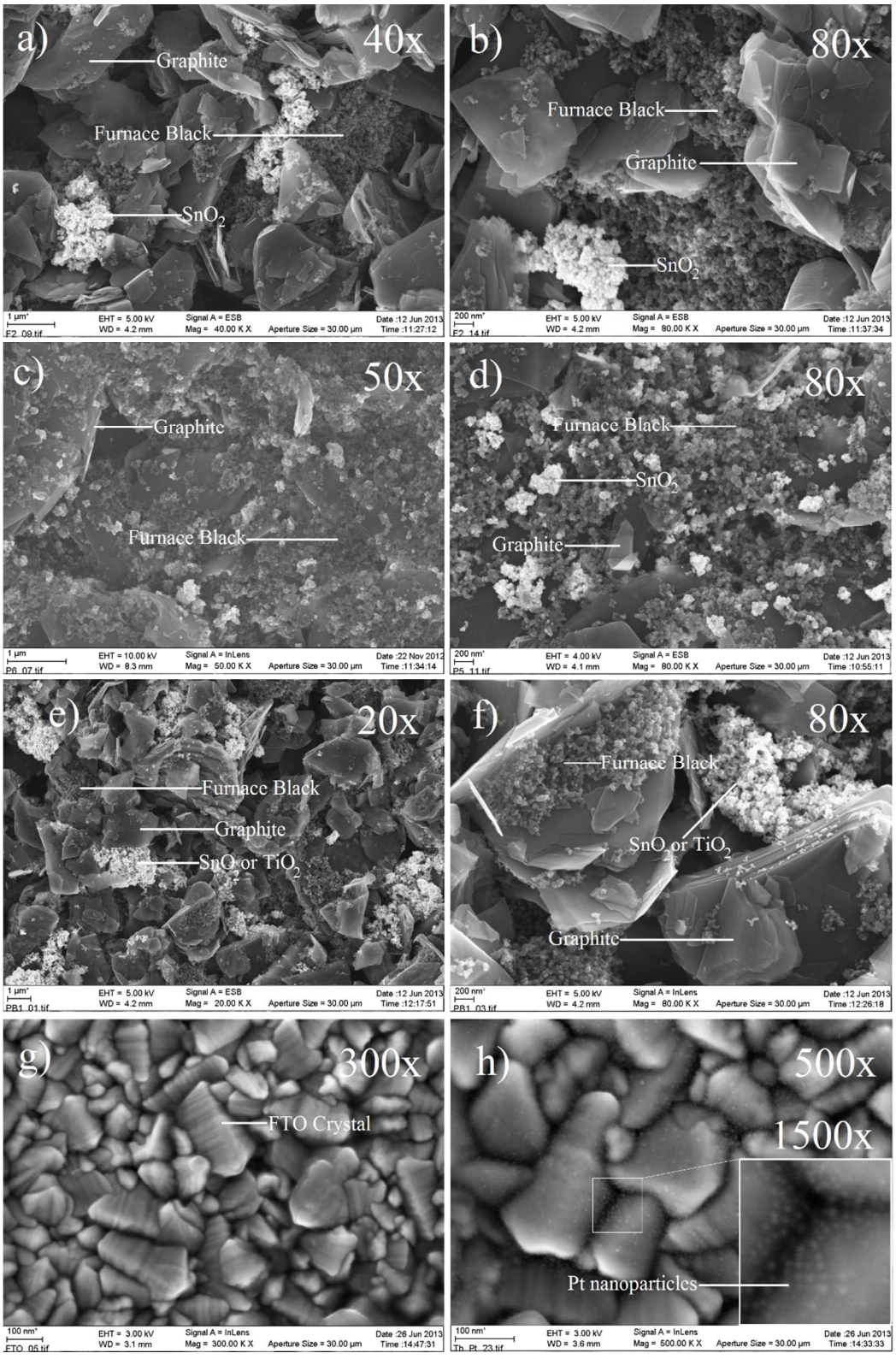


**Figure1**: SEM images of different carbon composites (a,b) BFCC, (c,d) PCC, (e,f) BCC, (g) Bare FTO-glass (h) Thermally platinized CE. BCC=Binder carbon composite, PCC=PEDOT carbon composite, BFCC=Binder free carbon composite.

*3.2 Mechanical stability of carbon composites*

The mechanical elasticity and stability of deposited layers will depend on how well the layers adhere to the substrate. In our earlier studies lower short circuit current densities were observed in case of PEDOT catalyst layer presumed to be caused by detachment of PEDOT particles and their settlement on PEs [5]. Moreover a lower fill factor was obtained due to gelator which demonstrated a tradeoff between the adhesion and photovoltaic performance of carbon catalyst layer based DSC [18]. It therefore seems that mechanical stability is not only important from the perspective of durability in handling and manufacturing of the DSSC but may also affect indirectly the photovoltaic parameters e.g. the short circuit current density $J_{SC}$, the fill factor (FF) or the total cell resistance ($R_{cell}$) of the cells.

Figure S1 (a-f) (see supporting information) [19] represents the elastic behavior of all the studied carbon composites on ITO-PEN and ITO-PET upon bending. The flaking of the particles in case of low temperature inks is well-known in DSSCs. Keeping this problem in mind every composite was grinded in a ball mill for 2 hours. The ball milling step is known to increase the surface areas of the deposited layers by breaking down the particles.

All three types of carbon composites (BFCC, PCC and BCC) exhibited high degree of flexibility (4 mm bending radius) and reproducibility on ITO-PEN sheets with no visual cracking or flaking of the particles (Figure S1 a-c). The ball milling of the particle was essential to avoid cracking and flaking upon bending.

On the other hand, surprising result was obtained in case of ITO-PET sheets loaded with BCC where the adhesion was found significantly lower than with ITOPET-PCC and ITOPET-BFCC electrodes (Figure S1 f). The BCC catalyst layer flaked off upon slight bending of the substrates. Nevertheless the ITOPET-BFCC and ITOPET-PCC showed similar flexibility as on the ITO-PEN sheet (Figure S1 d, e).

The adhesion of carbon composites deposited on FTO Glass, ITO-PEN and ITO-PET substrate was also studied with a tape test as given in the supporting information (Figure S2) [19]. Without going into quantitative analysis, these results are illustrated with photographs (Figure S2) [19] and also summarized in Table 1.

The adhesion behavior of the carbon composites has been categorized into three groups (Table 1). In most of the cases only small fractions (10-30%) of the catalyst layers were removed upon pulling of the tape Table 1, (Figure S2 f, h, j, n, p,) [19] which ensures the good overall adhesion of the films. Additionally in the best cases FTO Glass-PCC and ITOPET-BCC combinations), only few particles of the deposited layers were detached Table 1, (Figure S2 d, r,) [19] whereas in the worst cases (FTO Glass-BFCC and ITO PEN-BCC combinations) the catalyst layers were almost completely (98%) removed from the substrate Table 1, (Figure S2 b, l,) [19].

The PCC catalyst layers deposited on FTO-Glass, ITO-PEN and ITO-PET substrates exhibited better adhesion (Fig. S2 d, j, p) than other types of catalyst layers which may be a result of good bonding of the PEDOT polymer with the substrates. Best adhesion result of the PCC catalyst layer was obtained on the FTO-Glass in which case only a few particles (~ 1%) were transferred on the tape (Figure S2 d).

In case of plastic substrates, the BCC catalyst layer showed best adhesion on ITO-PET where only a very small part (~ 2%) of the catalyst layer was detached, but unexpectedly, the same (BCC) catalyst layer was completely peeled off from ITO-PEN in the tape test (Figure S2 l) Presumably the $TiO_2$ nanoparticles, used in the composite as binder particles, failed to make firm enough bonding with the ITO-PEN substrate but bonded reasonably well on ITO-PET. Similarly poor adhesion behavior was obtained also with the BFCC-FTO Glass combination where almost all the catalyst layer was almost completely transferred on the tape (Figure S2 b), which demonstrates the need for binder materials in the composites.

**Table 1:** Adhesion characteristics of carbon composites deposited on FTO Glass, ITO-PEN and ITO-PET Sheets.

| Substrate / Catalyst* | Dominant way of detachment of the film from the substrate | | |
|---|---|---|---|
| | Particles from film | Parts of the film ( 10-30%) | Most of the film (> 90%) |
| FTO Glass-BFCC | | | X |
| FTO Glass-PCC | X | | |
| FTO Glass-BCC | | X | |
| ITO PEN-BFCC | | X | |
| ITO PEN- PCC | | X | |
| ITO PEN-BCC | | | X |
| ITO PET-BFCC | | X | |
| ITO PET-PCC | | X | |
| ITO PET-BCC | X | | |

*FTO=Fluorine doped tin oxide, ITO=Indium doped tin oxide, PEN= Polyethylenenaphtalate, PET=Polyethyleneterephtalate, CE=Counter electrode, PE=Photoelectrode, BCC=Binder carbon composite, PCC=PEDOT carbon composite, BFCC=Binder free carbon composite.

*3.3 Photovoltaic performance*

Table 2 represents the average photovoltaic parameters of DSC cells illuminated and recorded from the photoelectrode (PE) side, classified according to the type of composite. It should be noted that in this study, no black tape mask (usually recommended to minimize the coupling of diffuse light into the cell) was used due to its firmly sticking over the cells which was causing a detachment of the flexible substrates. As a result, these test solar cells collected more light (from non-normal angles) in our solar simulator, compared to the reference silicon solar cells used for light intensity calibration and consequently the reported short circuit current densities are indeed over estimations of the current densities that would be obtained with actual direct beam sunlight. This overestimation was separately determined to be 2-8% depending on the cell type (results not shown) however, a correction for this overestimation was not performed since the focus of the study was on the counter electrodes (CEs) performance which in principle affect only Fill Factor (*FF*) but not short circuit current density ($J_{SC}$). The effect of < 10% offset in the effective light intensity compared to exact calibration can be considered to have a negligible effect on *FF*. Additionally the three times applied $TiCl_4$ treatment of the $TiO_2$ films in the present case is also well known to enhance $J_{SC}$ [20]. Hence all the cells exhibited relatively high short circuit densities ($J_{SC}$ ~ 18 mA/cm$^2$, Table 2) compared to our previous studies [5].

However the BFCC catalyst layer CEs on ITO-PEN exhibited significantly lower current densities (15 mA/cm$^2$). A possible reason can be the detachment of catalyst particles from the CE and their settling on the PE. Loosely bonded particles may be mixed with the electrolyte and transfer to the PE and reduce its performance by increasing electron transfer to the electrolyte (recombination). We have previously reported this in the case of PEDOT-TsO CEs observed as a

decrease in the electron collection efficiency deduced from the comparison of IPCE ratios [5]. However, in the present case such analysis is not possible since the carbon composite film is opaque and PE cannot be illuminated through the CE side, as needed in the IPCE-ratio method. Nevertheless the tape adhesion test section supports the possibility of detachment of loosely bonded particles.

Also, a lower cell resistance (average $R_{cell}$ = 12.5 Ωcm$^2$) was observed in completely rigid cells (grey and light blue rows in Table 1) compared to ITO-PEN ($R_{cell}$ = 18 Ωcm$^2$) and ITO-PET ($R_{cell}$ = 19 Ωcm$^2$) based CEs. All plastic cells had also a lower fill factor (ITO-PEN = 46 %, ITO-PET = 42%) than the FTO-glass cells (~ 53 %). The higher $R_{cell}$ and lower *FF* in case of ITO-PET is expected based on its higher sheet resistance (60 Ω/□). However as the ITO-PEN has equal sheet resistance as FTO-Glass (15 Ω/□), its higher $R_{cell}$ and lower *FF* must be due to some other reason, presumably due to weak adhesion i.e. poor contact of the carbon composites particles with the ITO layer and therefore higher contact resistance. Variations in $R_{cell}$ can also affect the *FF* [5].

The $R_{cell}$ consists of several factors such as the charge transfer resistance ($R_{CT}$) at the counter electrode, ideality of the photoelectrode, sheet resistance ($R_{SH}$) of the substrate, resistivity of the electrical contacts, and diffusion in the electrolyte [5]. However, due to similar materials and preparation techniques used, only the charge transfer resistance and the sheet resistance should be the main causes for differences in the $R_{cell}$ [5]. A detailed analysis of these is presented in Chapters 3.4 and 3.5.

Considering cell efficiencies on FTO glass, the binder-free carbon composite (BFCC) exhibited the highest efficiency (6.5 ± 0.1%); for comparison PCC 6.2 ± 0.4% and BCC 5.6 ± 0.4%. In case of plastics, the highest efficiency was obtained on ITO-PEN with BCC (5.9 ± 0.3%) along with PCC (5.6 ± 0.2%) and BFCC (5.1 ± 0.6%). These performances are comparable to the reference cells with thermally platinized counter electrodes (7 ± 0.2%).

**Table 2:** Photovoltaic performances of the cells. The $R_{cell}$ is the inverse of the slope of IV curve at open circuit.

| Type of Paste | Cell Type* | $J_{SC}$ (mA/cm$^2$) | $V_{OC}$ (mV) | *FF* (%) | $\eta$ (%) | $R_{cell}$ (Ωcm$^2$) |
|---|---|---|---|---|---|---|
| | Reference $G_{PE}$-$G_{CE}$ | 17.8 ± 0.5 | 717 ± 17 | 55 ± 2 | 7.0 ± 0.2 | 12 ± 2 |
| BFCC (A) | $G_{PE}$-$G_{CE}$ | 17.9 ± 0.7 | 680 ± 18 | 54 ± 4 | 6.5 ± 0.1 | 11 ± 1 |
| | $G_{PE}$-$PEN_{CE}$ | 15.8 ± 1.0 | 727 ± 15 | 43 ± 4 | 5.1 ± 0.6 | 20 ± 2 |
| | $G_{PE}$-$PET_{CE}$ | 17.6 ± 0.4 | 693 ± 20 | 40 ± 5 | 4.9 ± 0.9 | 21 ± 4 |
| PCC (B) | $G_{PE}$-$G_{CE}$ | 17.0 ± 2.0 | 711 ± 16 | 53 ± 1 | 6.2 ± 0.4 | 13 ± 2 |
| | $G_{PE}$-$PEN_{CE}$ | 17.0 ± 0.4 | 673 ± 10 | 49 ± 3 | 5.6 ± 0.2 | 16 ± 2 |
| | $G_{PE}$-$PET_{CE}$ | 17.7 ± 0.6 | 659 ± 11 | 44 ± 2 | 5.1 ± 0.1 | 17 ± 1 |
| BCC (C) | $G_{PE}$-$G_{CE}$ | 17.2 ± 0.2 | 667 ± 16 | 49 ± 2 | 5.6 ± 0.4 | 14 ± 1 |
| | $G_{PE}$-$PEN_{CE}$ | 17.7 ± 0.5 | 729 ± 13 | 46 ± 3 | 5.9 ± 0.3 | 17 ± 2 |
| | $G_{PE}$-$PET_{CE}$ | 17.8 ± 0.9 | 710 ± 16 | 42 ± 4 | 5.1 ± 0.4 | 19 ± 5 |

G=Glass, PEN=Polyethylenenaphtalate, PET=Polyethyleneterephtalate, CE=Counter electrode, PE=Photoelectrode, BCC=Binder carbon composite, PCC=PEDOT carbon composite, BFCC=Binder free carbon composite. "The measurements were made without a masking the cell, which overestimates the $J_{SC}$ by 2-8% compared to a situation with a mask. (See text for further discussion)."

*3.4 Electrochemical Impedance Spectra of DSSC*

Figure 2 represents typical EIS spectra of complete DSSC engineered with PEDOT-carbon composite (PCC) counter electrodes on FTO-glass, ITO-PET and ITO-PEN. All measurements were performed under 1 Sun light intensity (1000 W/m$^2$) and open circuit voltage conditions. The EIS frequency range was from 100 mHz to 100 kHz. In this frequency range the reference DSSC based on a thermally platinized glass counter electrode exhibits three impedance arcs, two

in the lower frequency range, i.e. around 1 Hz and 20-30 Hz (Fig. 2 b) which correspond to the diffusion resistance ($R_D$ = 1 Ωcm$^2$) and the electron recombination resistance ($R_{REC}$ = 3.6 Ωcm$^2$) respectively, and one in the higher frequency (> 1 kHz) which corresponds to the charge transfer resistance ($R_{CT}$ = 4.9 Ωcm$^2$) at the counter electrode.

The PEDOT carbon composite (PCC) based catalyst layer resulted in a large semicircle with glass (3.8 Ωcm$^2$), ITO-PET (4.5 Ωcm$^2$) and ITO-PEN (4.1 Ωcm$^2$) CEs (Fig2 a). These large semicircles represent the responses of the PE and CE in the low frequency region (~10-20 Hz), which overlap and form one large semicircle instead of two individual ones [5, 18]. Hence it is difficult to estimate the exact value of $R_{CT}$ from Fig. 2 in case of a porous carbon based CE. One way to estimate $R_{CT}$ is to subtract $R_{REC}$ from the value since the PE geometry was the same (0.4 cm$^2$).

Small semicircles adjacent to the large ones are evident in all carbon based cells (Fig.2 a: Glass-PCC = 1.3 Ωcm$^2$, ITOPET-PCC = 2.0 Ωcm$^2$, ITOPEN-PCC = 1.5 Ωcm$^2$) which corresponds to very high frequency (~ 10 kHz) peak and could be associated with a second Nernst diffusion impedance resulted from diffusion through the pores of carbon composite as reported by others [21]. The values of these extra semicircles were added to the charge transfer resistance to get the total charge transfer resistance ($R_{CE\text{-}total}$) [5, 18].

Table 3 summarizes the resistance values calculated with the aforementioned assumptions. Only the PEDOT carbon composite (PCC) is discussed here to understand the restrictions for calculating the accurate $R_{CT}$ values. The impedance spectra of all three types of carbon composites will be discussed in more detail in Chapter 3.5.

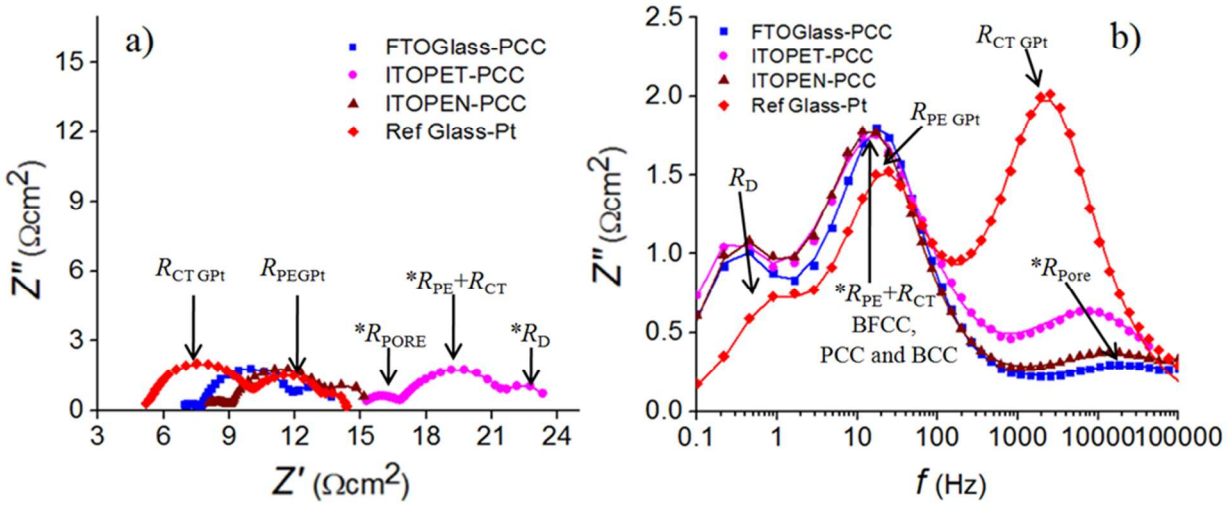


**Figure 2:** Typical EIS spectra of complete DSSCs with PEDOT-carbon composite (PCC) catalyst layer counter electrodes on glass, ITO-PET, ITO-PEN and a reference thermally platinized counter electrode on glass. a) Nyquist plots b) Imaginary impedance Z'' vs frequency. *These impedances positions are also valid for FTO-Glass PCC and ITO-PEN PCC.

**Table3:** Typical $R_S$, $R_{CT}$ and $R_{CE\text{-}total}$ values of FTO-Glass, ITO-PEN and ITO-PET with PEDOT- carbon composite (PCC). $R_{CE\text{-}total}$ includes the charge transfer resistance and the in-pore diffusion resistance values.

| Type of CE / Catalyst | $R_S$(Ωcm$^2$) | $R_{CT}$ (Ωcm$^2$) | $R_{CE\text{-}total}$ (Ωcm$^2$) |
|---|---|---|---|
| FTO Glass / PCC | 6.5 | 0.2 | 1.5 |
| ITO-PEN / PCC | 7.6 | 0.3 | 1.8 |
| ITO-PET / PCC | 14.8 | 0.7 | 2.7 |
| Glass / Pt (reference) | 5.1 | 4.9 | 4.9 |

$R_S$=Series resistance, $R_{CT}$=Charge transfer resistance, $R_{CE\text{-}total}$=Total charge transfer resistance = $R_{pore}$ + $R_{CT}$ for carbon counter electrodes, Pt=Platinum.

The highest $R_S$ (14.8 Ωcm$^2$, Table 2) was found with the ITO-PET CE as expected due to the large sheet resistance ($R_{SH}$ = 60 Ω/□) of the substrate as compared to 15 Ω/□ for the ITO-PEN and FTO glass substrates. The reference thermally platinized counter had the lowest $R_S$ (5.1 Ωcm$^2$).

Nevertheless, the catalytic activity of all PCC based CEs on every type of substrate outclassed the thermally platinized CE. The total charge transfer resistance ($R_{CE\ total}$) of Glass-PCC based CE was less than one-third (1.5 $\Omega cm^2$) of the thermally platinized CE (4.9 $\Omega cm^2$ Table 3). The ITO-PEN-PCC CE gave almost the same (1.8 $\Omega cm^2$) but the ITO-PET-PCC CE had almost a double value (2.7 $\Omega cm^2$). We presume that the higher surface area along with a reasonably conductive carbon composite catalyst layers combined with the catalytic activity of PEDOT:PSS caused such a high catalytic performance.

*3.5 CE-CE cell configuration*

To gain more accurate information of the charge transfer resistance, we also employed a CE-CE cell [22-24]. The CE-CE configuration eliminates all possible responses from the PE side [24]. Figure 3 represents typical EIS responses of three different carbon composites based CE-CE cells. These measurements were carried out at room temperature with 10 mV voltage amplitude and zero volts DC.

The two frequency peaks are clearly evident for all porous carbon CEs; one in the lower (~ 10-100 Hz) and the other in the higher frequency range (~ 100 kHz). These are associated with the charge transfer resistance and the in-pore diffusion resistance respectively (Fig.3 b). This reinforces also our earlier observation about the overlapping PE and CE semicircles in the DSSC meaning that the peak must be associated with the porous carbon CE as here we have no PE. The thermally platinized glass CE-CE cell exhibited two frequency peaks at similar positions than in the complete DSSC cell corresponding to recombination resistance ($R_{REC}$) and diffusion resistance ($R_D$). It should be noted that only CE-CE- PCC cell configuration exhibited the $R_D$ peak due to a thinner layer of bulk electrolyte in case of CCCEs and secondly the diffusion

impedance is smaller because of the porous structure evens out surface concentrations difference. As a result, the impedance peak in Figure 3 b decreases and moves to the higher frequencies making it indistinguishable in the spectrum.

All the different composite based CE-CE cell assemblies exhibited almost the same $R_S$ (BFCC = 3.1 $\Omega cm^2$, PCC = 3.0 $\Omega cm^2$ and BCC = 3.1 $\Omega cm^2$ obtained from Fig. 3a). This also proves that the variations in the $R_S$ of the complete DSSCs were cause by different sheet resistances of the CE substrates (FTO Glass was used at the both sides of the CE-CE cells).

The $R_{CT}$ of the BCC based CE-CE cell is lower (2 $\Omega cm^2$) than that of the BFCC (3.3 $\Omega cm^2$) and the PCC (2.8 $\Omega cm^2$), even though the width of the semicircles that corresponds to the in-pore diffusion resistance was almost same (~ 1 $\Omega cm^2$). The carbon-based catalyst layers showed very low $R_{CT}$ compared to the thermally platinized CE (4 $\Omega cm^2$). This performance was expected as suggested earlier in section 3.1 where the SEM images revealed high active surface area of the carbon composites as compare to thermally platinized catalyst layer. The total charge transfer resistance ($R_{CE\text{-}total}$) and the series resistances of the samples are summarized in Table 4.

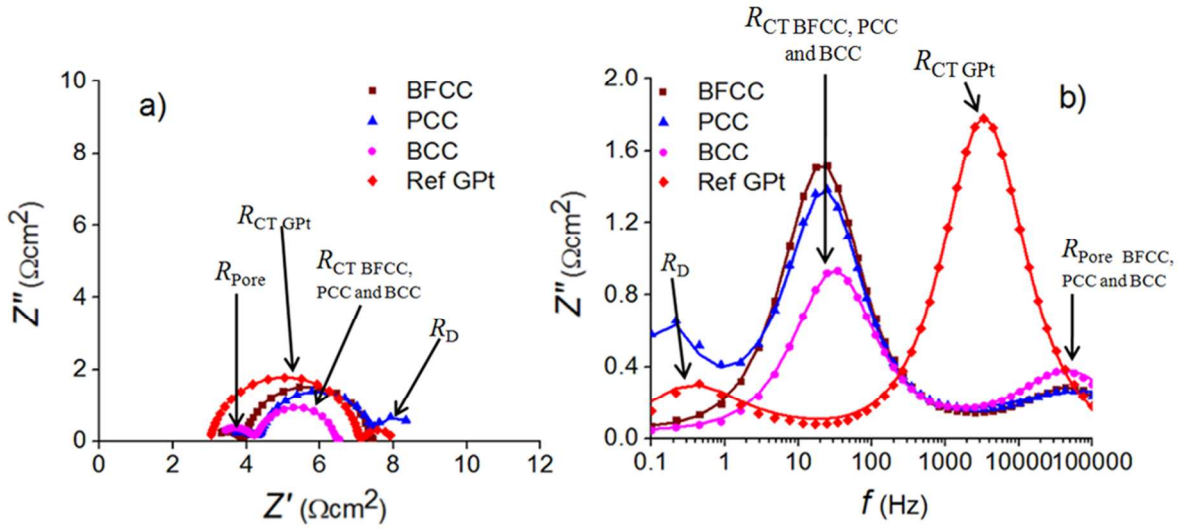


**Figure 3:** EIS spectra of CE-CE configuration a) Nyquist plots b) Imaginary Impedance Z'' as a function of frequency. The values presented here are calculated for one counter electrode. BFCC=Binder free carbon composite, PCC=PEDOT carbon composite, BCC=Binder carbon composite.

**Table 4:** $R_S$, $R_{CT}$ and $R_{CE\text{-}total}$ values of CE-CE cell configuration loaded with BFCC, PCC and BCC composites. $R_{CE\text{-}total}$ includes the charge transfer resistance and the in-pore diffusion resistance values.

| Type of Catalyst | $R_S$ ($\Omega cm^2$) | $R_{CT}$ ($\Omega cm^2$) | $R_{CE\text{-}total}$ ($\Omega cm^2$) | $C_{CE}$ ($\mu F cm^{-2}$) | $R_{CT}C_{CE}$ ($\mu s$) |
|---|---|---|---|---|---|
| (BFCC) | 3.1 | 3.3 | 3.9 | 3002 | 9906 |
| (PCC) | 3.0 | 2.8 | 3.8 | 2759 | 7725 |
| (BCC) | 3.1 | 2.0 | 3.0 | 3603 | 7206 |
| (Reference G Pt) | 3.0 | 4.0 | 4.0 | 14 | 56 |

$R_S$=Series resistance, $R_{CT}$=Charge transfer resistance, $R_{CE\text{-}total}$=Total charge transfer resistance.

*3.6 Active surface area and catalytic activity*

In our previous publication [17] we devised a method for quantitative relative comparison of the catalytic activity of different catalyst particles materials. According to the method, the product of the measured charge transfer resistance ($R_{CT}$) and electrochemical double layer capacitance ($C_{CE}$)

of the counter electrode, in other words the RC time-constant of the electrode, can be used as figure of merit for the catalytic activity. This is because both the effect of film thickness and active surface area per unit volume on $R_{CT}$ and $C_{CE}$ cancel out when calculating their product that becomes $R_{CT}*C_{CE} = r_{CT}*c_{CE}$, where $r_{CT}$ is the charge transfer resistance per microscopic surface area of the catalyst (measure of the catalytic activity of that catalyst particle surface) and $c_{CE}$ is the double layer capacitance per unit volume of the electrode. Relative comparison of $r_{CT}$ becomes thus possible in terms of the measured values of the product $R_{CT}*C_{CE}$, if $c_{CE}$ can be assumed similar in all cases, which we think is a reasonable assumption at least among the different carbon composite formulations due to similar base materials (graphite, furnace black, $SnO_2$).

Table 4 lists the calculated values for $C_{CE}$ and $R_{CT}*C_{CE}$ in different cases. The two orders of magnitude difference in the $C_{CE}$ between the carbon composites and the thermal Pt counter electrode demonstrates the substantially larger active surface area per electrode area of the former. On the other hand, the catalytic activity, indicated by the product $R_{CT}*C_{CE}$ is two orders of magnitudes lower for the carbon composites than for Pt. The higher active surface are of the carbon composite electrode thus fully compensates for the lower catalytic activity of the carbon materials they are made of and renders the catalytic performance of the prepared thick and porous electrodes ($R_{CT}$) similar or slightly better than the almost planar Pt CEs. The catalytic activities ($R_{CT}*C_{CE}$) observed here for the different carbon composites are in the same order as the values obtained for our previous carbon composite CEs, and CEs based on single-walled carbon nanotube thin films and multi-walled carbon nanotube "forests" [17]. This observation underlines our previous conclusion [17] that engineering a good carbon based CE for DSSC is possible by dense enough packing of the carbon catalyst material to thick enough film to meet

the requirement for $R_{CT}$ (1 - 5 $\Omega cm^2$). The present work additionally demonstrates that the high performance of such carbon electrodes can be maintained by modification of the carbon paste formulation and preparation method while improving the flexibility and adhesion of the composite films on the flexible substrates.

## 4. Conclusion

Different types of carbon composites based counter electrodes (CE) have been analyzed in this study. CEs with very good catalytic activity were demonstrated. In a complete cell configuration, PEDOT carbon composites had lower charge transfer resistances (~ 1.5 – 3 $\Omega cm^2$) than the reference cell with traditional thermally platinized counter electrodes (5 $\Omega cm^2$). Among plastic cells, the highest efficiency (~ 6 %) was recorded with binder enriched carbon composite catalyst layers which was only slightly lower than that of the reference DSSC (7%). The same catalyst layer out-performed the reference Pt and other carbon composites catalyst layers in a CE-CE configuration and exhibited low charge transfer resistance (3 $\Omega cm^2$). The mechanical stability of the plastic carbon composite CEs were good. The study suggests a great potential of employing these composites as a replacement of the traditional expensive Pt catalyst layer in a flexible or roll to roll produced DSSC.

## Acknowledgment

This work was financed through a project National Consortium for Low Cost Photovoltaic from the Academy of Finland. Mr. Ghufran Hashmi thanks Mr. Sami Vasala, Mr Erno Kemppainen and Dr Imran Asghar for the useful discussions during the work and Mr Antti Ruuskanen for the help in cell assembly.

## References

[1] G. Hashmi, K. Miettunen, T. Peltola, J. Halme, I. Asghar, K. Aitola, M. Toivola, and P. Lund, *Renew. Sust. Energ. Rev.,* 2011, **15**, 3717-3732.

[2] T. Ma, X. Fang, M. Akiyama, K. Inoue, H. Noma and E. Abe, *J. Electroanal. Chem.,* 2004, **574**, 77–83.

[3] M. G. Kang, N. Park, K. S. Ryu, S. H. Chang, K. Kim, *Sol. Energy Mater. Sol. Cells.,* 2006, **903**, 574–581.

[4] T. Miyasaka, M. Ikegami, Y. Kijitori, *J. Electrochem. Soc.,* 2007, **154**, A455-461.

[5] G. Hashmi, K. Miettunen, J. Halme, I. Asghar, H. Vahlman, T. Saukkonen, Z. Huaijin, P. Lund, *J. Electrochem. Soc.,* 2012, **159,** H656-H661.

[6] L. Yi, Y. Liu, N. Yang, Z. Tang, H. Zhao, G. Ma, Z. Sua and D. Wang, Energy Environ. Sci., 2013, 6, 835–840.

[7] A. Hauch and A. Georg, *Electrochim. Acta.*, 2001, **46**, 3457–3466.

[8] H. Lee, M. W. Horn, Sculptured platinum nanowire counter electrodes for dye-sensitized solar cells, Thin Solid Films (Article in Press; http://dx.doi.org/10.1016/j.tsf.2013.04.079)

[9] M. Toivola, J. Halme, K. Miettunen, K. Aitola, P. Lund, Int J Energy Res 2009, 33, 1145–60.

[10] W. Zeng, G. Fang, X. Wang, Q. Zheng, B. Li, H. Huang, H. Tao, N. Liu, W. Xie, X. Zhao, D. Zou, J. Power Sources 2013, 229, 102-111.

[11] S. H. Park, H.R. Jung, W. J. Lee, Electrochim Acta., 2013, **102**, 423– 428.

[12] X. Miao, K. Pan, Q. Pan, W. Zhou, L. Wang, Y. Liao, G. Tian, G. Wang, Electrochimica Acta 2013, **96**, 155– 163

[13] M. Xu, G. Liu, X. Li, H. Wang, Y. Rong, Z. Ku, M. Hu, Y. Yang, L. Liu, T. Liu, J. Chen, H. Han, Organic Electronics 14 (2013) 628–634

[14] H. Pettersson, T. Gruszecki, C. Schnetz, M. Streit, Y. Xu, L. Sun, et al, *Prog Photovolt: Res Appl.,* 2010, **18**, 340–345.

[15] L. Kavan, J. H. Yum, M. K. Nazeeruddin, M. Grätzel, *ACS Nano*., 2011 **11**, 9171-9178.

[16] T. N. Murakami, M. Gratzel. *Inorg Chim Acta.,* 2008, **361**,572–80.

[17] K. Aitola. J. Halme, N. Halonen, A. Kaskela, M. Toivola, A. G. Nasibulin, K. Kordás, G. Tóth, E. I. Kauppinen, P. Lund, Thin Solid Films 519 (2011) 8125–8134.

[18] K. Miettunen, M. Toivola, G. Hashmi, J. Salpakari, I. Asghar, P. Lund, Carbon., 2011, **49**, 528-532.

[19] Supporting Information.

[20] S. Ito, T. N. Murakami, P. Comte, P. Liska, C. Grätzel, Mohammad. K. Nazeeruddin, M. Grätzel, *Thin Solid Films.,* 2008, **516**, 4613–4619.

[21] J. D. Roy-Mayhew, D.J. Bozym, C. Punckt, I.A. Aksay, ACS Nano 4 (2010) 6203–6211

[22] N. Papageorgiou, W. F. Maier, M. Grätzel, *J. Electrochem. Soc.,* 1997, **144**, 876–884.

[23] Y. Saito, W. Kubo, T. Kitamura, Y. Wada, S. Yanagida, *J. Photochem. Photobiol. A: Chem.,* 2004, **164**, 153–157.

[24] J. Halme, M. Toivola, A. Tolvanen, P. Lund. *Sol. Energy Mater. Sol. Cells*., 2006, **90**, 872–86.

[25] http://www.ipc.org/TM/2.4.1E.pdf

[26] http://www.pstc.org/files/public/101.pdf